KSME Journal, Vol. 2, No. 1, pp. 69~78, 1988.

THE MECHANICAL EFFICIENCY AND KINEMATICS OF PANTOGRAPH-TYPE MANIPULATORS

Shin-Min Song* and Jong-Kil Lee*

(*Received May, 7, 1988*)

Pantograph mechanism has been well known for its motion feature of decoupled kinematics. Planar pantograph mechanism has been extensively used in machinery since the seventeenth century. Recently, three dimensional pantographs have been used in walking machine leg and manipulator designs. This is because, the pantograph mechanism possesses the following advantages decoupled kinematics, higher energy efficiency, good rigidity, less link inertia and compact drive systems. In this paper, the mechanical efficiency of the kinematics of pantograph type manipulators are studied. The mechanical efficiency of pantograph mechanisms and conventional open-chain and closed-chain type manipulators are studied and evaluated using the concept of modified geometric work. The kinematics of six-d.o.f., pantograph type manipulators are studied and special mechanisms which simplify the kinematics are introduced. The computational complexity of both Cartesian and cylindrical type pantograph manipulators are evaluated and compared with a PUMA type manipulator.

Key Words: Pantograph Mechanism, Mechanical Efficiency, Inverse Position Analysis

1. INTRODUCTION

In a strict sense, the term pantograph mechanism is reserved for a special type of five-link mechanism (see Fig. 1) which possesses a decoupled kinematic relationship between the output motion of the reference point F and the two input degrees of motion. The closed-chain structure is a parallelogram and points A, B and F are maintained collinear at all times. The driving points of the two input degrees of freedom can be respectively assigned to points A and B, or they can be both assigned to either one of these two points. If the two input degrees of motion are driven separately by two linear actuators which are parallel with the two axes of the reference coordinate system, the kinematic relationship between input and output motion becomes decoupled. This type of pantograph mechanism, which was called simple pantogrpah in (Song, Lee and Waldrom, 1987) has been extensively used in embroidering machines, copying machines and magnifying mechanisms since the seventeenth century. Later, in the nineteenth century, a more general form of pantograph, the skew pantograph or the plagiograph, as it was called by its inventor, was introduced by Sylvester (Hobson, et al., 1953). Referring to Figure 2, the skew pantograph is obtained by attaching two similar triangulated rigid links to the parallelogram ACDE. If one carefully arranges the orientation of the two input linear axes with respect to the reference coordinate system, a decoupled kinematic relationship which is similar to that of the simple pantographs can be obtained. The way to define the orientation of the input linear axes was shown in (Song, Lee and Waldron, 1987) and will be reviewed in a later section.

Although both the simple and skew pantographs are planar mechanisms, they can be extended to a three-dimensional mechanism by the following two methods: The first method is to mount the frame on the base via a revolute joint (see Fig.

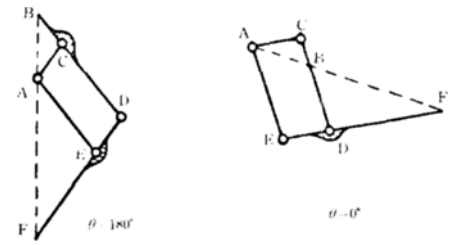

Fig. 1 Simple pantographs

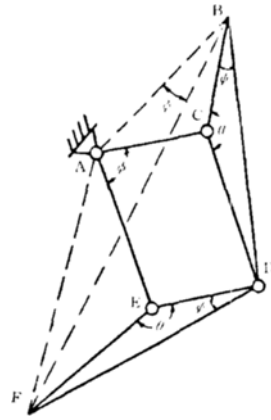

Fig. 2 A skew pantograph

*Department of Mechanical Engineering, University of Illinois at Chicago, Chicago, Illinois 60680, U.S.A.

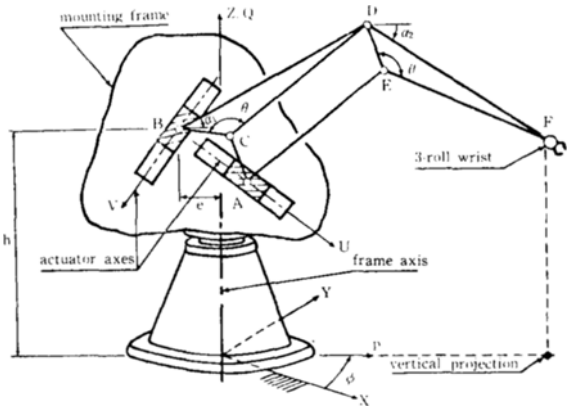

Fig. 3 A cylindrical type pantograph manipulator

3). If the axis of the revolute joint is in the plane which contains the planar pantograph, the mechanism has decoupled kinematics in a cylindrical coordinate system. This type of pantograph is called a cylindrical pantograph. The second method is to mount the two input points A and B on a pair of revolute joints which have their axes parallel to one another (see Fig. 4). Thus, a lateral movement of one input point will cause the pantograph to stretch and rotate simultaneously, and the motion of the output point becomes three dimensional. Although a skew pantograph can generate three-dimensional motion, it was shown in (Song, Lee and Waldron, 1987) that only the simple pantographs have decoupled kinematics in Cartesian coordinate system. This type of three-dimensional pantograph is called Cartesian type pantograph and was first introduced by Hirose and Umetani in (Hirose and Umetani, 1980). They designed a quadrupedal walking machine with four Cartesian type pantograph legs.

In recent years, pantograph mechanisms have been frequently used in the robotics area, such as in the design of walking machine legs (Hirose and Umetani, 1980; Hirose, 1984; Kesseis, Rambaut and Penne, 1981; Song, Waldron and Kinzel, 1985) and manipulators (GAC Corp., 1982; Song and Lin, 1987; Yang and Lin, 1985). This is because, in addition to decoupled kinematics, this ancient mechanism possesses many other important advantages. These advantages include a high mechanical efficiency, high payload/weight ratio, low link inertia and compact drive systems. The high mechanical energy efficiency is because no geometric work is consumed during operation. This will be explained in detail in a later section. The high payload/weight ratio is due to the closed-chain structure of a pantograph. The low link inertia is because the actuators are mounted low on the rotating base. The compact size of the drive systems are due to the magnification motion feature of pantographs. Because of these advantages, pantograph mechanisms are especially suitable for the applications of walking machines, where computational efficiency of inverse kinematics and dynamics (Song, lee and Waldron, 1987), energy efficiency and mechanical strength are important. Since the demands on computational and mechanical efficiencies of manipulators are becoming more strict, pantograph mechanisms will be more attractive in future manipulator design.

Although some of the advantages of pantograph mechanisms have been scatteredly mentioned in literature (Hirose and Umetani, 1980; Hirose, 1984; Hobson, et. al., 1953; Song, Waldron and Kinzel, 1985; Song and Lin, 1987; Yang and Lin, 1985), the advantages of high mechanical efficiency and decoupled kinematics were not fully investigated. Hence, it is the goal of this paper to present to the readers a complete study of these two aspects. In the following, the basic kinematics of Cartesian and cylindrical pantographs is reviewed first. The mechanical efficiency of the pantograph is then studied and compared with other types of manipulators. The kinematics of a six-d.o.f. pantograph type manipulators are is then studied in detail. Two wrist mechanisms which can simplify the kinematic relationships are also discussed.

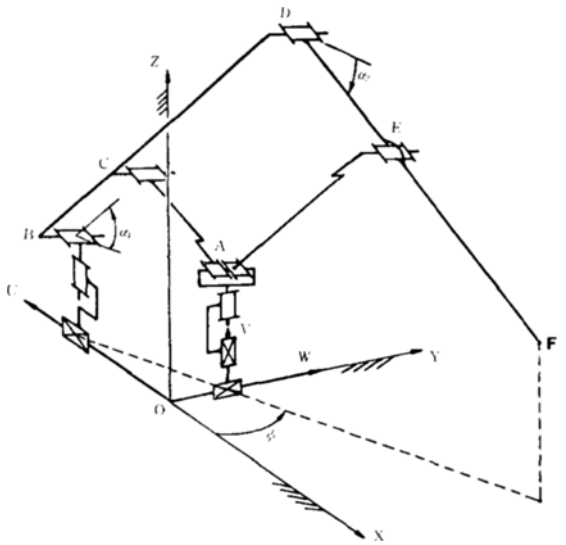

Fig. 4 Schematic diagram of a three-d.o.f. Cartesian type pantograph

2. BASIC KINEMATIC FEATURES OF PANTOGRAPHS

The basic kinematic features of pantographs are reviewed in this section. Figure 2 shows a skew pantograph mechanism. The angle θ is called the skew angle. ACDE is a parallelogram and BCD and DEF are two similar triangulated links. It has been proven that ΔABF is similar to either ΔBCD or ΔDEF as long as ACDE is kept a parallelogram (Hobson, et. al., 1953). Thus, the motion of a pantograph can be fully represented by the imaginary, dashed triangle ABF, which was called equivalent triangle in (Song, Waldron and Kinzel, 1985). That is, given the positions of points A and B, the position of point F can be obtained by constructing the equivalent triangle.

The fundamental motion feature of a skew pantograph is stated as: If point A is fixed and point B traces a given curve, then point F traces a similar curve. The magnitude of the curve is magnified by a ratio R and the orientation is rotated through the skew angle θ with respect to the given curve. Similarly, if point B is fixed and point A traces a given curve, then point F traces a given curve, The magnitude of the curve is magnified by a ratio R' and the orientation is rotated through an angle ψ with respect to the given curve, where

$$R=\frac{AF}{AB},\quad R'=\frac{BF}{AB}=(1+R^2-2R\cdot\cos\theta)^{\frac{1}{2}} \tag{1}$$

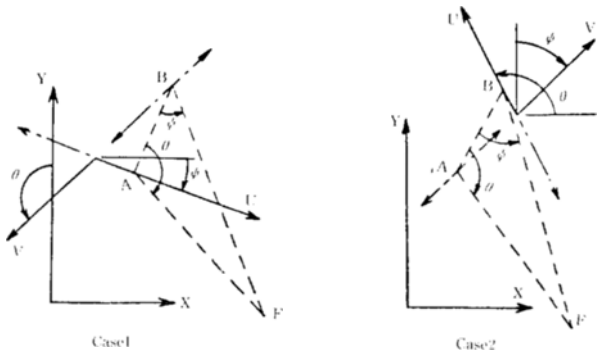

Fig. 5 Principal axes and actuator arrangements of 2D pantograph

$$\psi = \tan^{-1}\left(\frac{R \cdot \sin\theta}{R_1}\right) \tag{2}$$

Based on the concept of equivalent triangle, several sets of principal axes were defined in (Song, Lee and Waldron, 1987). If the actuators are mounted in line with the principal axes, the kinematic equations of input points and reference point F are fully decoupled. Referring to Case 1 of Fig. 5, points A and B are the input points for the X-and Y-movements of point F, respectively. The U-axis is obtained by rotating the X-axis by an angle of $-\psi$ and the V-axis is obtained by rotating the Y-axis by an angle of θ V-and V-axes are the principal axes of this case. In Case 2, points A and B are the input points for the Y-and X-movements of point F, respectively. The U-axis is obtained by rotating X-axis by an angle of $-\theta$ and V-axis is obtained by rotating Y-axis by an angle of $-\psi$. Similarly, one can also define the principal axes for the cases where both input degrees of motion are assigned to just one input point (either A or B). When the skew angle θ becomes 0° or 180°, the pantograph geometries become the simple pantographs in Fig. 1.

In the following, the kinematics of both Cartesian and cylindrical type pantographs are reviewed:

2.1 Cartesian Type

Referring to Fig. 4, the forward and inverse kinematics of the Cartesian type pantograph have very simple forms. Since only a simple pantograph can be constructed as a Cartesian type pantograph, the skew angle is selected as 180° for discussions. From Eq. (1), $\theta = 180°$ gives $R' = R + 1$. Referring to Fig. 4, the forward position equations are:

$$\begin{bmatrix} X_f \\ Y_f \\ Z_f \end{bmatrix} = \begin{bmatrix} R & 0 & 0 \\ 0 & (R+1) & 0 \\ 0 & 0 & (R+1) \end{bmatrix} \begin{bmatrix} U \\ W \\ V \end{bmatrix} \tag{3}$$

where X_f, Y_f and Z_f are the coordinates of the hand reference point F; U, W and V are the linear displacements of the input points A and B along the three actuator axes. U and V are measured from the intersection of these two axes. W is measured from the intersection of U-and W-axes. The inverse position equations can be derived directly from Eq. (3) as follows:

$$\begin{bmatrix} U \\ W \\ V \end{bmatrix} = \begin{bmatrix} 1/R & 0 & 0 \\ 0 & 1/(R+1) & 0 \\ 0 & 0 & 1/(R+1) \end{bmatrix} \begin{bmatrix} X_f \\ Y_f \\ Z_f \end{bmatrix} \tag{4}$$

As is apparent, all the d.o.f. are fully decoupled. The inverse velocity and acceleration equations can be easily obtained by taking the first and second derivatives of Eq. (4), respectively.

2.2 Cylindrical Type

A three-d.o.f, cylindrical type pantograph manipulator is shown in Fig. 3. A cylindrical coordinate system (P, Q, ϕ) is chosen as the reference frame to describe the motion of the hand reference point F. The forward position equations can be derived as:

$$\begin{bmatrix} P \\ Q \\ \phi \end{bmatrix} = \begin{bmatrix} R' & 0 & 0 \\ 0 & R & 0 \\ 0 & 0 & 1 \end{bmatrix} \begin{bmatrix} U \\ V \\ \phi \end{bmatrix} + \begin{bmatrix} e \\ h \\ 0 \end{bmatrix} \tag{5}$$

where (P, Q, ϕ) is the coordinates of point F; U and V are respectively the displacements of the two input points A and B and are measured from the intersection of the two principal axes; e and h are the offsets of the intersection along P and Q axes, respectively. The inverse position equations can be obtained as:

$$\begin{bmatrix} U \\ V \\ \phi \end{bmatrix} = \begin{bmatrix} 1/R' & 0 & 0 \\ 0 & 1/R & 0 \\ 0 & 0 & 1 \end{bmatrix} \begin{bmatrix} P \\ Q \\ \phi \end{bmatrix} + \begin{bmatrix} -e/R' \\ -h/R \\ 0 \end{bmatrix} \tag{6}$$

Again, all the d.o.f. are fully decoupled. The inverse velocity and acceleration equations can be obtained by taking the first and second derivatives of Eq. (6), respectively.

If the hand reference point is deviated from the point F, the complexity of kinematics will increase tremendously. Hence, the main advantage of the pantograph manipulator is compromised and such a deviation of the hand reference point should be avoided.

3. MECHANICAL EFFICIENCY

That a pantograph type walking machine leg possesses a very high mechanical efficiency was shown by Hirose and Umetani in Hirose and Umetani, (1980). They pointed out that the high mechanical efficiency was due to a gravitationlly decoupled actuator (GDA) system used in the pantograph leg. That is, the actuators are geometrically decoupled between the gravitational direction and its perpendicular direction. Any robot which uses a GDA system, such as a conventional Cartesian manipulator, has high mechanical efficiency. They also explained the inefficiency of an open-chain walking machine leg. But they did not provide any numerical measurement to evaluate the mechanical efficiency of a robotic system. In (Waldrom and Kinzel, 1981) Waldron and Kinzel discussed about the relationship between actuator geometry and mechanical efficiency in robots. They pointed out that the efficiencies of most robots of this generation were very low. The reason for the low efficiencies were largely due to the actuators' acting as brakes; i.e., they are "back-driven". They termed the energy lost when the actuator acts as a brake as geometric work. They illustrate the concept of geometric work using a force-distance diagram of one linear actuator after it executes through a complete cycle (see Fig. 6). The lower part (shaded area) is negative work (the distance is reducing) and was called geometric work. The white area is the net output work. Although the concept of geomet-

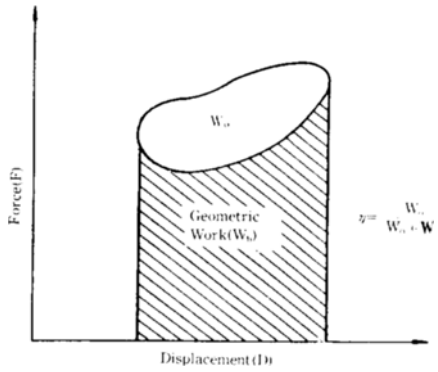

Fig. 6 Relationship of geometric work W_b, output work W_o, and mechanical efficiency η as viewed on a full cycle plot of actuator force F versus displacement D. Redrawn from Waldron and Kinzel (1981)

ric work was very helpful to understand the poor efficiency of many robots, the definition of geometric work was somewhat ambiguous because of the following reasons: First, the geometric work should be related to all the actuators in one system, not just one actuator. Second, not all negative works are geometric work and some positive works can also be geometric work. This will be explained shortly. Here we redefine the geometric work as the sum of the absolute values of the works consumed by all actuators of one robotic system subtracted by the absoulte value of the output work done by the system to the environment. Thus we can combine geometric work and output work to calculate the mechanial efficiency of a robotic system as:

$$\text{Mechanical Efficiency} = \frac{\text{Output Work}}{\text{Output Work} + \text{Geometric Work}} \tag{7}$$

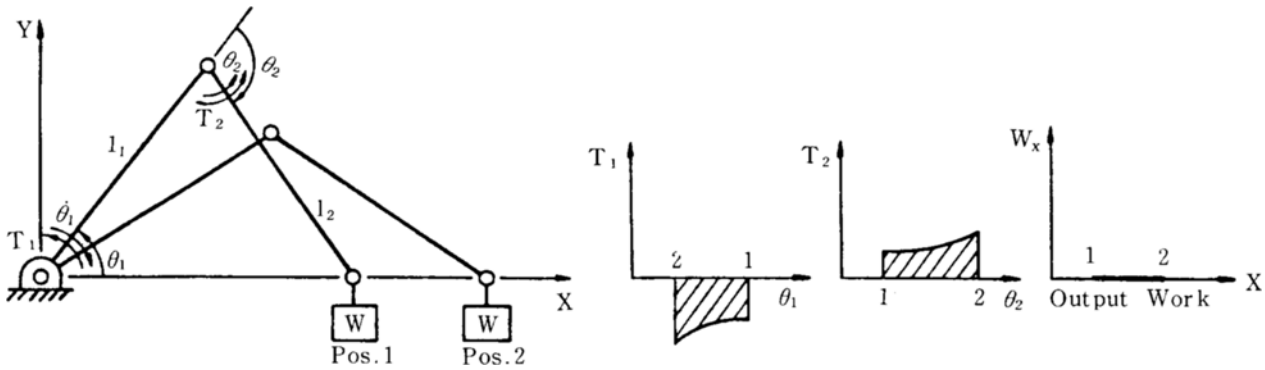

$T_1 = W \cdot (l_1 \cos\theta_1 + l_2 \cos(\theta_1 + \theta_2))$
$T_2 = W \cdot l_2 \cos(\theta_1 + \theta_2)$

(a) Open-chain manipulator

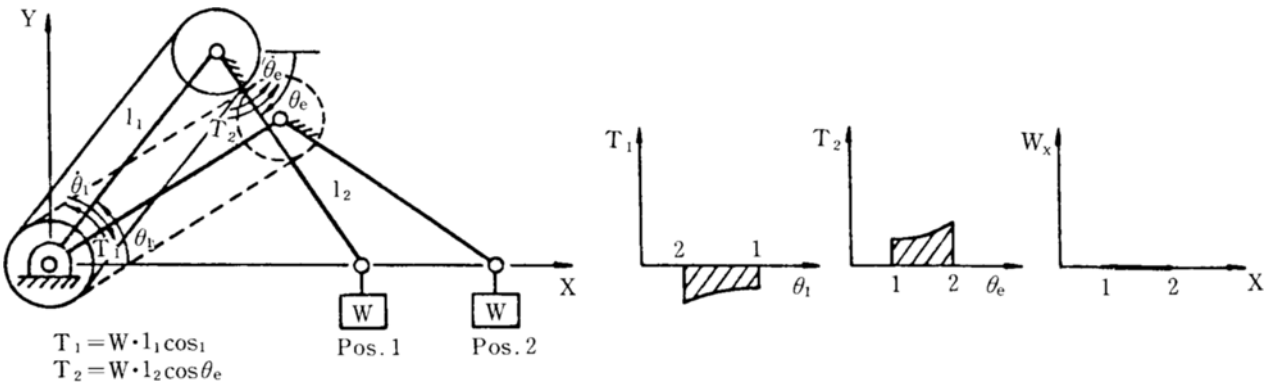

$T_1 = W \cdot l_1 \cos\theta_1$
$T_2 = W \cdot l_2 \cos\theta_e$

(b) Open-chain manipulator with pulley and chain system

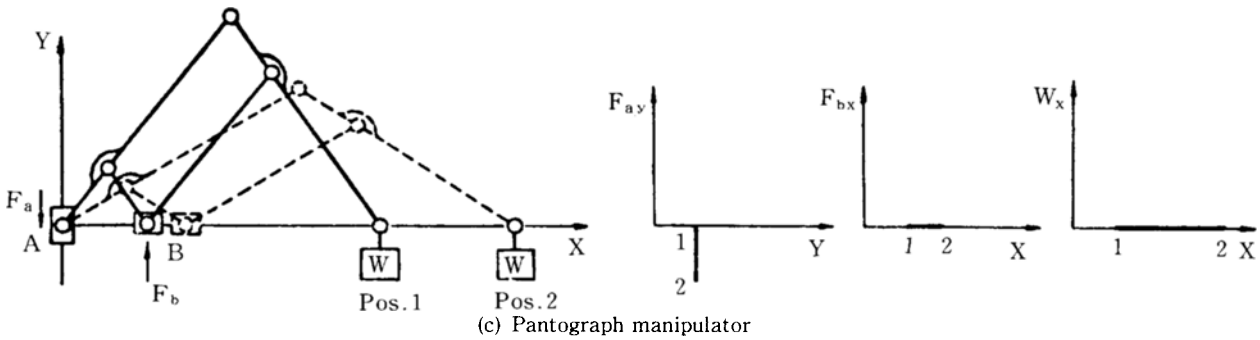

(c) Pantograph manipulator

Fig. 7 Mechanical efficiency of three types of manipulator along a horizontal path

Hence, the greater the geometric work is, the lower the mechanical efficiency is. In the following, we will apply this redefined geometric work to evaluate the mechanical efficiency of a pantograph mechanism and compare it with a conventional open-chain and closed-chain manipulators.

Let us first consider the geometric work of a two-link open-chain manipulator. Referring to Fig. 7 (a), the end-effector is moving from position 1 to 2 along a horizontal

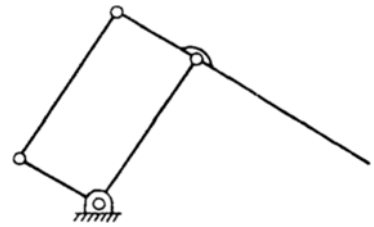

Fig. 8 A parallelogram five-link mechanism

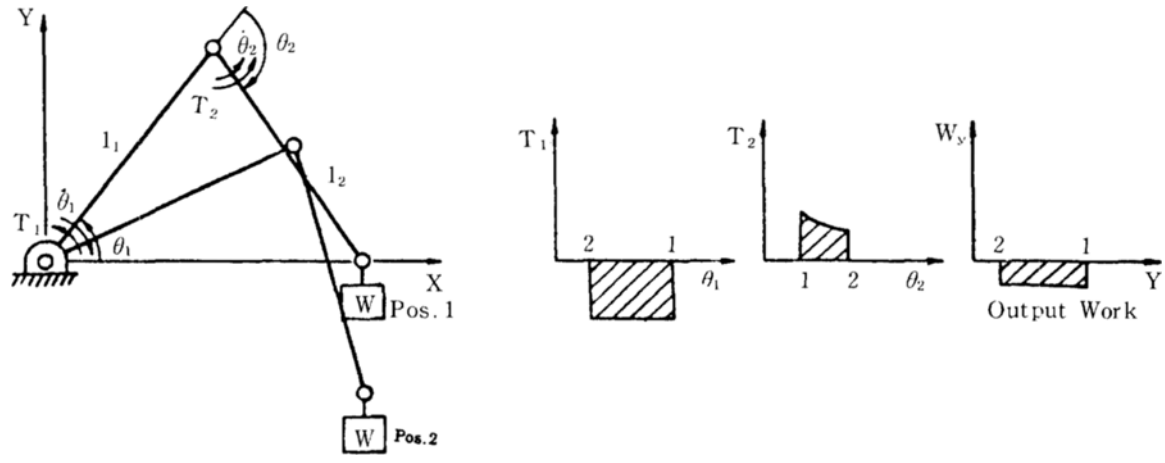

$T_1 = W \cdot (l_1 \cos\theta_1 + l_2 \cos(\theta_1 + \theta_2))$
$T_2 = W \cdot l_2 (\theta_1 + \theta_2)$

(a) Open-chain manipulator

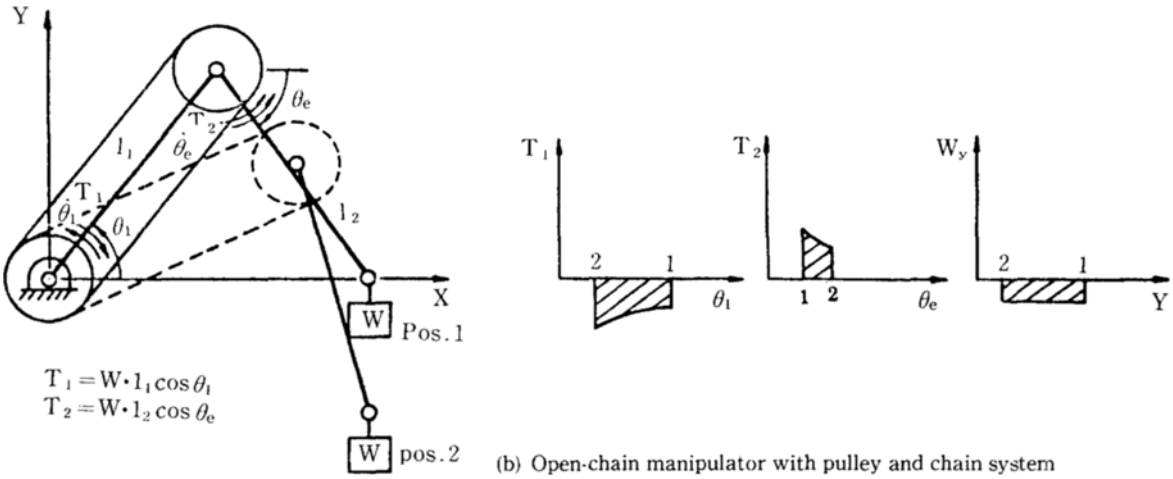

$T_1 = W \cdot l_1 \cos\theta_1$
$T_2 = W \cdot l_2 \cos\theta_e$

(b) Open-chain manipulator with pulley and chain system

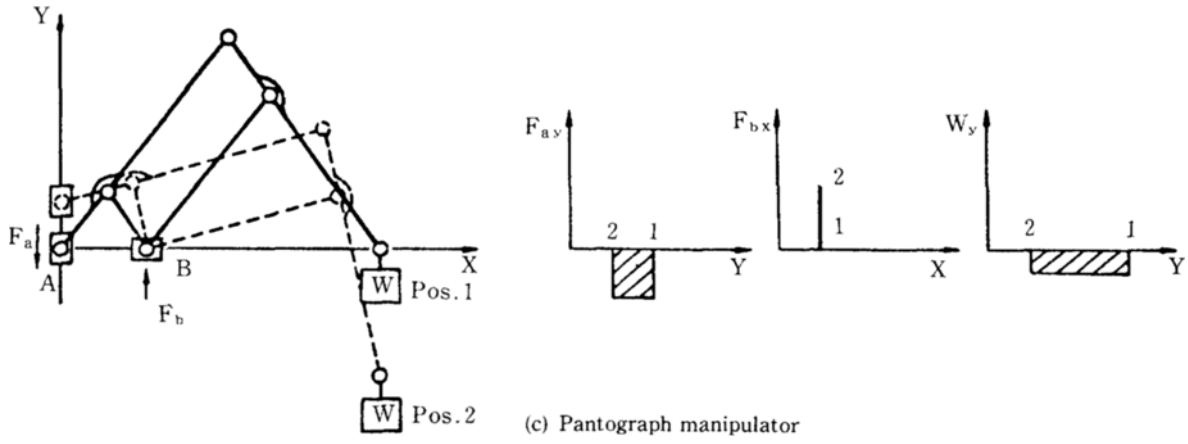

(c) Pantograph manipulator

Fig. 9 Mechanical efficiency of three types of manipulator along a vertical path

path with a constant speed. We assume that the system is frictionless; the two links are weightless and only the object carried by the end-effector has significant weight. Since there is no change in the energy state of the object, the output work done by the manipulator to the object is zero. The motor at the base joint is acting as a brake and doing negative work because the output torque is in the opposite direction of the motor motion. The motor at the elbow joint is doing positive work. The overall works done by these two motors are shown in Fig. 7 (a). The area under T_1 should be equal to the area under T_2 since the sum of them is equal to the output work which is zero. This also means that all the positive work done by the elbow motor is entirely consumed by the base motor as negative work. Both the positive and negative works contribute no output work and are related to the geometry of the manipulator. Hence, the sum of the absolute values of these two works is the geometric work of the system. Now, referring to Fig. 7 (b), if we mount a pulley and chain system on the two joints and move the elbow motor to the base to be co-axial with the base motor, the geometric work of the system is reduced. This is because the torque at joint 2 is transmitted to the elbow motor through the chain system and the torque at the base motor becomes $W \cdot l_1 \cos\theta_1$. The angular displacement of the elbow motor is also changed. Hence, we can improve the mechanical efficiency of the two-link system by adding such a chain and pulley system. The improvement will be even greater if we consider the weight of the elbow motor in the calculation. Now, if we replace the chain and pulley system with a parallelogram as it is shown in Fig. 8, the geometric work remains unchanged. The function of the parallelogram is kinematically equivalent to the pully and chain system. Now, let us consider the case of a pantograph manipulator. Referring to Fig. 7 (c), the vertical actuator is fixed and doing no work. The horizontal actuator is moving frictionlessly and also doing no work. Thus, geometric work is zero.

Let us consider the case that the end-effector is moving downward along a vertical path. For the open-chain manipulator, referring to Fig. 9 (a), the base motor is doing negative work and the elbow motor is doing positive work. The output work is negative since the potential energy of the object is reduced. Since the sum of the negative and positive works of the two motors should be equal to the negative output work, the geometric work is equal to twice the positive work of the elbow motor. For the open-chain manipulator with pulley and chain system, the geometric work is reduced due to the above-mentioned reason [see Fig. 9 (b)]. The same situation is found in the closed-chain parallelogram manipulator. As for a pantograph manipulator, referring to Fig. 9 (c), the horizontal actuator is fixed and doing no work and the veritical actuator is doing negative work. Since the amount of the negative work is equal to the negative output work, the geometric work is zero. Hence, we may conclude that a closed-chain manipulator (or an open-chain manipulator with pulley and chain system) has better mechanical efficiency than an open-chain manipulator and a pantograph type manipulator has the best mechanical efficiency of all type 1 actuators.

4. KINEMATICS OF SIX-D.O.F. PANTOGRAPH MANIPULATORS

We have seen the kinematics of three-dimensional pantographs in a previous section. In this section, we will discuss about the kinematics of six-d.o.f. pantograph type manipulators. A six-d.o.f. pantograph type manipulator can be obtained by attaching a three-roll wrist at the end link of a three-dimensional pantograph. The wrist center should be coincident with the point F in order to have a simpler kinematic relationship. For a six-d.o.f., Cartesian type pantograph manipulator (referring to Fig. 4), the inverse position, velocity and acceleration analyses of the first three axes (U, V and W) are very simple since these three degrees of freedom are fully decoupled. The analyses of the last three axes (θ_4, θ_5 and θ_6), however, are not that simple due to the following reasons: The wrist experiences a pitching motion when either one or both of the first two axes (U and V) move. That is, the angle α_2 changes. Also, the wrist experiences both a pitching and yawing when the third axis W moves. This is, both α_2 and ϕ change. Since these pitching and yawing motions as well as the last three joint axes affect the orientation of the wrist, the inverse position analysis of the last three axes is more complicated. The inverse velocity and acceleration analyses become very complicated because the first and second derivatives of the angle α_2 have very complicated forms [refer to Eq. (51) in Appendix]. Thus, the advantage of simple kinematics diminishes. Hirose and Umetani introduced a pair of differential mechanisms which can eliminate the unwanted pitching and yawing motions of the wrist due to the motions of the first three axes (Hirose and Umetani, 1980). After some modification this pair of differential mechanisms is drawn in Fig. 10. During motion, the bottom bevel gear at joint U does not rotate and, if both motors 4 and 5 are stationary, the yawing motion of the wrist is eliminated by the motion of the differential mechanism. Moreover, the pitching motion is eliminated by the parallelogram motion performed through the pulley and chain system. Hence, the kinematics of the last three d.o.f. is fully decoupled from the first three d.o.f.. The derivation of the kinematic of equations is straightforward and is not presented here. The other advantage of this mechanism is that Motors 4 and 5, which control the pitching and yawing motion of the wrist through the differential mechanism, are mounted low so that the wrist inertia is reduced.

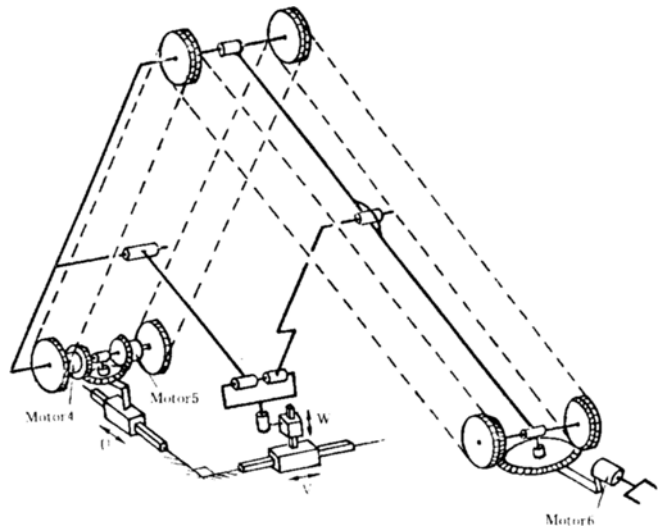

Fig. 10 A six-d.o.f. Cartesian type pantograph manipulator with a pair of differential mechanisms

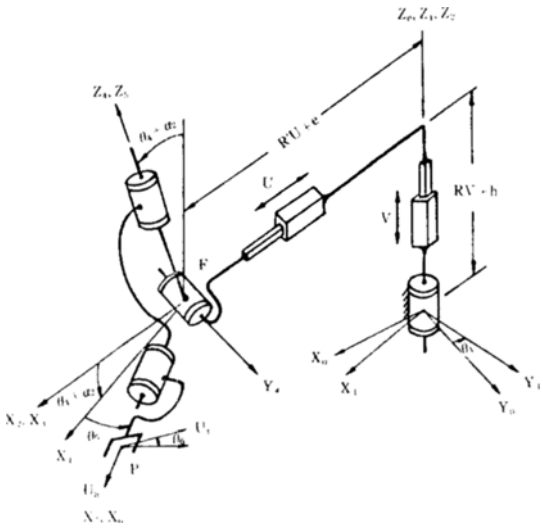

Fig. 11 A kinematic model of a six-d.o.f. cylindrical type pantograph manipulator at a general position

For the six-d.o.f., cylindrical type pantograph manipulator, the kinematics is somewhat more complicated and deserves a detailed study. Figure 11 shows a kinematic model of a six-d.o.f., cylindrical type pantograph manipulator at a general position. The closed-chain pantograph mechanism is now replaced by two independent prismatic joints. The vertical and horizontal prismatic joints generate a vertical displacement VR and a horizontal displacement UR' of the end-effector, respectively. Since R and R' are known constants, the actual input variables U and V can be easily obtained from these two joint variables. The pitching motion of the wrist due to the linear motions along the U and/or V axes is temporarily not considered here and will be included in the kinematics of the wrist. (At this point we should emphasize that this model does not exactly represent the cylindrical pantograph if we forget to include this pitching motion in the wrist kinematics. The reason we adopt this model is that the closed-chain geometry of the pantogrpah can be treated as an open-chain geometry for easy visualization.) The first wirst axis, joint 4 in the figure, is mounted to be perpendicular to the plane defined by the two prismatic joint axes so that the pitching angle α_2 due to U and/or V axes can be included in the rotational angle of axis 4. (That is, the actual rotation about axis 4 is $\alpha_2+\theta_4$ although the joint variable of joint 4 is θ_4 alone.) If the axis 4 is not mounted in the above-mentioned direction, an additional coordinated transformation is needed and the results become more complicated. This special arrangement of axis 4 becomes unnecessary if a parallelogram (pulley and chain) mechanism is added to the manipulator (see Fig. 12). The parallelogram motion eliminates the unwanted pitching motion of the wrist due to the motion along U and/or V axes. Joints 5 and 6 are set up in a way such that the three wrist axes are orthogonal and intersect at the concurrent point F. Let us first consider the case of a six-d.o.f., cylindrical type pantograph manipulator without a parallelogram mechanism.

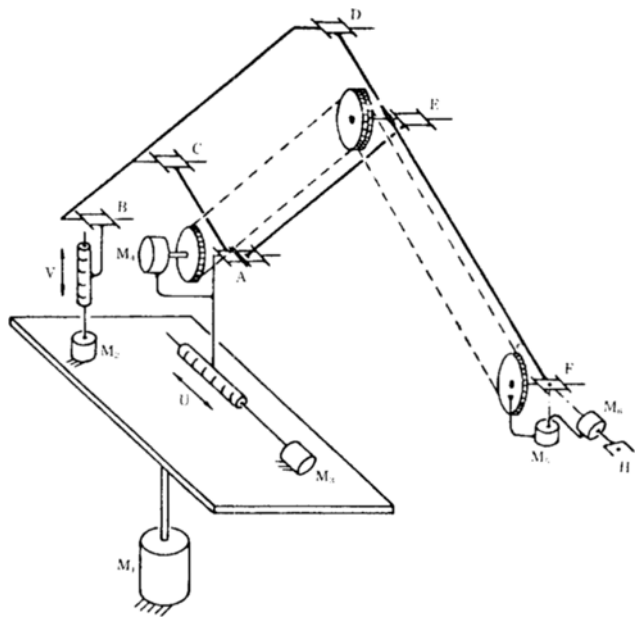

Fig. 12 A six-d.o.f. cylindrical type pantograph manipulator with a parallelogram mechanism

4.1 Inverse Position Analysis

While standard methods such as the Denavit-Hartenburg and zero position notation (Gupta, 1981) methods can be applied to derive the inverse position equations, we adopt the following method which was introduced by Hunt (1986) because it takes least efforts to obtain the solutions. This method allows us to derive the inverse position equations by direct observation.

Referring to Fig. 11, the hand position is specified by the position of point P and the axial and transverse hand vectors, namely U_a and U_t, respectively. The position of wrist center F can be computed as

$$\overline{F}=\overline{H}-d\bar{u}_a \tag{8}$$

Also, we can easily write down the coordinates of $0_6(0_5)$, which is located at wrist center, and the direction cosines of the hand axial axis, namely u_{ax}, u_{ay} and u_{az}, by direct inspection of Fig. 11.

$$X_f=(UR'+e)\cos\theta_1 \tag{9}$$

$$Y_f=(UR'+e)\sin\theta_1 \tag{10}$$

$$Z_f=VR+h \tag{11}$$

$$u_{ax}=\cos\theta_1\cos(\theta_4+\alpha_2)\cos\theta_5-\sin\theta_1\sin\theta_5 \tag{12}$$

$$u_{ay}=\sin\theta_1\cos(\theta_4+\alpha_2)\cos\theta_5+\cos\theta_1\sin\theta_5 \tag{13}$$

$$u_{az}=-\sin(\theta_4+\alpha_2)\cos\theta_5 \tag{14}$$

The angle α_2 can be computed according to Eq. (51) in the Appendix. The first three input variables θ_1, U and V can be obtained from Eqs. (9)~(11) as:

$$\theta_1=\tan^{-1}\left(\frac{Y_f}{X_f}\right) \tag{15}$$

$$U=\frac{1}{R_1}(X_f\cos\theta_1+Y_f\sin\theta_1-e) \tag{16}$$

$$V=\frac{1}{R}(Z_f-h) \tag{17}$$

Eliminating the terms which contain $\theta_4+\alpha_2$ in Eqs. (12), (13) leads to the following solution of joint angle θ^5:

$$\theta^5=\sin^{-1}(u_{ay}\cos\theta_1-u_{ax}\sin\theta_1) \tag{18}$$

Hence, we have two solutions of θ_5. Now, eliminating the terms which contain θ_5 in Eqs. (12)~(14) gives the solutions of $\cos(\theta_4+\alpha_2)$ and $\sin(\theta_4+\alpha_2)$ as:

$$\cos(\theta_4+\alpha_2)=\frac{u_{ax}\cos\theta_1+u_{ay}\sin\theta_1}{\cos\theta_5} \tag{19}$$

$$\sin(\theta_4+\alpha_2)=-\frac{u_{az}}{\cos\theta_5} \tag{20}$$

This gives

$$\theta_4=-\alpha_2+\tan^{-1}\left(\frac{\sin(\theta_4+\alpha_2)}{\cos(\theta_4+\alpha_2)}\right) \tag{21}$$

The transverse vector u_t is used to calculated θ_6. Vector u_t can be related to the unit vector j by the following corrdinated transformations:

$$\bar{u}_t=R_1R_2R_3R_4R_5R_6\,\bar{j} \tag{22}$$

where $\bar{j}=(0,1,0)^t$ and R_i's are the rotation matrices which can be constructed according to the coordinate systems. It should be noticed that the coordinate systems are not set up according to the Denavit-Hartenburg notation.

$$[R_1]=\begin{bmatrix}\cos\theta_1 & -\sin\theta_1 & 0\\ \sin\theta_1 & \cos\theta_1 & 0\\ 0 & 0 & 1\end{bmatrix},\quad [R_2]=[R_3]=\begin{bmatrix}1&0&0\\0&1&0\\0&0&1\end{bmatrix},$$

$$[R_4]=\begin{bmatrix}\cos\delta & 0 & \sin\delta\\ 0 & 1 & 0\\ -\sin\delta & 0 & \cos\delta\end{bmatrix}$$

$$[R_5]=\begin{bmatrix}\sin\theta_5 & -\sin\theta_5 & 0\\ \sin\theta_5 & \cos\theta_5 & 0\\ 0 & 0 & 1\end{bmatrix},\quad [R_6]=\begin{bmatrix}1 & 0 & 0\\ 0 & \cos\theta_6 & -\sin\theta_6\\ 0 & \sin\theta_6 & \cos\theta_6\end{bmatrix}$$

where $\delta=\theta_4+\alpha_2$. Multiplying both sides of Eq. (22) by $(R_1R_2R_3)^{-1}$ and expanding both sides gives three equations:

$$u_{tx}\cos\theta_1+u_{ty}\sin\theta_1=-\cos\delta\sin\theta_5\cos\theta_6+\sin\delta\sin\theta_6 \tag{23}$$

$$u_{tx}\sin\theta_1+u_{ty}\cos\theta_1=\cos\theta_5\cos\theta_6 \tag{24}$$

$$u_{tz}=\sin\delta\sin\theta_5\cos\theta_6+\cos\delta\sin\theta_6 \tag{25}$$

Eliminating the terms which contain θ_5 from Eqs. (23) and (25) gives the solution for $\sin\theta_6$, and $\cos\theta_6$ from Eq. (24) as:

$$\cos\theta_6=\frac{u_{tx}\sin\theta_1+u_{ty}\cos\theta_1}{\cos\theta_5} \tag{26}$$

$$\sin\theta_6=(u_{tx}\cos\theta_1+u_{ty}\sin\theta_1)\sin\delta+u_{tz}\cos\delta \tag{27}$$

$$\theta_6=\tan^{-1}\left(\frac{\sin\theta_6}{\cos\theta_6}\right) \tag{28}$$

4.2 Inverse Velocity Analysis

In a six degrees-of-freedom manipulator, the six joint rates ($\dot{q}_1-\dot{q}_6$) of a manipulator are related to the anglar velocity ($\bar{\omega}_h$) and linear velocity ($\bar{v}_h$) of the hand by a 6×6 Jacobian matrix $[J]$ (Whitney, 1972). The Jacobian matrix can be formed according to the following equation:

$$\begin{matrix}\\ i^{th}\ \text{col.}\\ \text{(prismatic)}\end{matrix}\quad\begin{matrix}\\ j^{th}\ \text{col.}\\ \text{(revolute)}\end{matrix}$$

$$\begin{bmatrix}\bar{\omega}_h\\ \bar{v}_h\end{bmatrix}_{6\times1}=\begin{bmatrix}0 & \bar{u}_j\\ \bar{u}_i & \bar{u}_j\times\overline{P_jH}\end{bmatrix}_{6\times6}\begin{bmatrix}\dot{q}_1\\ \vdots\\ \dot{q}_6\end{bmatrix}_{6\times1} \tag{29}$$

where u_i is the unit vector along joint i ; P_j is a point at joint j and H is a point at the hand. Vector $\overline{P_jH}$ is a vector from P_j to point H. The i^{th} column is applied to a revolute joint. In order to obtain a simple form of the Jacobian matrix, we will formulate the Jacobian matrix according to an imaginary point F which is attached at the hand and is coincident with the wrist center. The linear velocity of point F can be calculated from the known linear velocity at the tip of the hand as:

$$\bar{v}_f=\bar{v}_h-\bar{\omega}_h\times\bar{d} \tag{30}$$

Where d is the distance from wrist center to the hand point H. The angular velocity is the same for all points on the same rigid body. Hence,

$$\bar{\omega}_f=\bar{\omega}_h \tag{31}$$

Since the end-effector reference point is now selected at the wrist center where three axes are co-intersecting, the Jacobian matrix according to Eq. (29) becomes:

$$[J]=\begin{bmatrix}\bar{u}_1 & 0 & 0 & \bar{u}_4 & \bar{u}_5 & \bar{u}_6\\ \bar{u}_1\times\bar{r}_1 & \bar{u}_2 & \bar{u}_3 & 0 & 0 & 0\end{bmatrix} \tag{32}$$

where r_1 is the position vector of wrist point F in the fixed coordinate. Then by observation of Fig. 11 we can easily obtain the elements of Jacobian matrix as:

$$\begin{bmatrix}\bar{\omega}_f\\ \bar{v}_f\end{bmatrix}_{6\times1}=\begin{bmatrix}0 & 0 & 0 & -\sin\theta_1 & \cos\theta_1\sin\delta\\ 0 & 0 & 0 & \cos\theta_1 & \sin\theta_1\cos\delta\\ 1 & 0 & 0 & 0 & \cos\delta\\ -(R'U+e)\sin\theta_1 & 0 & R'\cos\theta_1 & 0 & 0\\ (R'U+e)\cos\theta_1 & 0 & R'\sin\theta_1 & 0 & 0\\ 0 & R & 0 & 0 & 0\end{bmatrix}\begin{bmatrix}\cos\theta_1\cos\delta\cos\theta_5-\sin\theta_1\sin\theta_5\\ \sin\theta_1\cos\delta\cos\theta_5+\cos\theta_1\sin\theta_5\\ -\sin\delta\cos\theta_5\\ 0\\ 0\\ 0\end{bmatrix}\begin{bmatrix}\dot{\theta}_1\\ \dot{V}\\ \dot{U}\\ \dot{\theta}_4\\ \dot{\theta}_5\\ \dot{\theta}_6\end{bmatrix} \tag{33}$$

It should be noticed that columns 2 and 3, respectively, are multiplied by constants R and R'. This is because the joint variables of these two joints were selected RV and $R'U$, respectively, and only $\dot{V}$ and $\dot{U}$ should remain in the 6×1 column vector. Now, we have to include the joint rate change

α_2 into the top three elements of columns 2 and 3 (Remember that the model in Fig. 11 does not exactly represent the motion of a pantograph.) In order to do this we have to differentiate α_2 [refer to Eq. (51) in Appendix]. The resultant equation is quite complicated and the terms of $\dot{U}$ and $\dot{V}$ are coupled together. We can set one of $\dot{U}$ and $\dot{V}$ to zero to obtain the relationship of $\dot{\alpha}_2$ and the other. Thus, we can obtain the following equation:

$$\dot{\alpha}_2 = A \cdot \dot{U} + B \cdot \dot{V} \tag{34}$$

where A and B are very lengthy coefficients. Finally, the Jacobian matrix of the six-d.o.f., cylindrical type manipulator is obtained by replacing the upper left 3×3 matrix of Eq. (33) with the following matrix:

$$\begin{bmatrix} 0 & -B\cdot\sin\theta_1 & -A\cdot\sin\theta_1 \\ 0 & B\cdot\cos\theta_1 & A\cdot\cos\theta_1 \\ 1 & 0 & 0 \end{bmatrix} \tag{35}$$

Since the computation of coefficients A and B are computationally inefficient, the simple kinematics of the three-dimensional cylindrical pantograph is no more maintained. Thus, from the point of view of computational efficiency, it is more advantageous to include a parallelogram mechanism into the system (see Fig. 12). The parallelogram motion through the pulley and chain system eliminates the unwanted pitching motion of the wrist. With such an inclusion, the Jacobian matrix of the six-d.o.f., cylindrical type pantagraph manipulator is exactly the same as in Eq. (33), except that the angle δ should be replaced with θ_4 since the angle α_2 is no more in existence. The inverse velocity analysis is obtained by multiplying Eq. (33) out:

$$\omega_{fx} = -\dot{\theta}_4\sin\theta_1 + \dot{\theta}_5\cos\theta_1\sin_4 + \dot{\theta}_6(\cos\theta_1\cos_4\cos\theta_5 - \sin\theta_1\sin\theta_5) \tag{36}$$

$$\omega_{fy} = +\dot{\theta}_4\sin\theta_1 + \dot{\theta}_5\sin\theta_1\sin_4 + \dot{\theta}_6(\sin\theta_1\cos_4\cos\theta_5 - \cos\theta_1\sin\theta_5) \tag{37}$$

$$\omega_{fz} = \dot{\theta}_1 + \dot{\theta}_5\cos_4 - \dot{\theta}_6\sin\theta_4\cos\theta_5 \tag{38}$$

$$v_{fx} = -\dot{\theta}_1(R'U + e)\sin\theta_1 + \dot{U}\,R'\cos\theta_1 \tag{39}$$

$$v_{fx} = \dot{\theta}_1(R'U + e)\cos\theta_1 + \dot{U}\,R'\sin\theta_1 \tag{40}$$

$$v_{fx} = R\cdot\dot{V} \tag{41}$$

The last three equations contains only $\dot{\theta}_1$, $\dot{V}$ and $\dot{U}$ and these three joint rates should be solved first. This gives

$$\dot{\theta}_1 = \frac{-v_{fx}\sin\theta_1 + v_{fy}\cos\theta_1}{R'U + e} \tag{42}$$

$$\dot{U} = \frac{v_{fx}\cos\theta_1 + v_{fy}\sin\theta_1}{R_1} \tag{43}$$

$$\dot{V} = \frac{v_{fz}}{R} \tag{44}$$

where v_{fx}, v_{fy} and v_{fz} are the three components of linear velocity of the end effector at point F. Finally, the last three joint rates are solved from Eq. (36) through (38) as:

$$\dot{\theta}_5 = (\omega_{fx}\cos\theta_1 + \omega_{fy}\sin\theta_1)\sin\theta_4 + (\omega_{fz} - \dot{\theta}_1)\cos\theta_4 \tag{45}$$

$$\dot{\theta}_6 = \frac{1}{\cos\theta_5}\{(\omega_{fx}\cos\theta_1 + \omega_{fy}\sin\theta_1)\cos\theta_4 - (\omega_{fz} - \dot{\theta}_1)\sin\theta_4\} \tag{46}$$

$$\dot{\theta}_4 = -\omega_{fx}\sin\theta_1 + \omega_{fy}\cos\theta_1 - \dot{\theta}_6\sin\theta_5 \tag{47}$$

4.3 COMPUTATIONAL COMPLEXITY

In order to get a feeling of the computational complexity of six-d.o.f. pantograph manipulators, the numbers of multiplications (divisions), additions (subtractions) and transcendental function calls of the inverse position and velocity analyses of the six-d.o.f., cylindrical type pantograph manipulator are mumerated and compared with those of a PUMA manipulator. These numbers are tabulated in Tables 1 and 2. In the enumeration, all the identical groups of variables which appear twice or more are only counted once and the division in all inverse tangent function call is not counted since the FORTRAM function ATAM2 is used in computer programming. The numbers of computations of the six-d.o.f., Cartesian type pantograph manipulator with the differential mechanism should be much less than the numbers of the cylindrical type manipulator listed in these tables.

Table 1 Computational complexity of inverse position analysis

Type	Multiplication/ division	Addition/ subtraction	Transcendental Function
PUMA (Hollerbach 1983)	64	38	10
PUMA (Paul 1986)	37	26	10
Cylindrical pantograph with parallelogram mechanism	20	11	7

Table 2 Computational complexity of inverse velocity analysis

Type	Multiplicaton/ division	Addition/ subtraction
PUMA (Hollerbach 1983)	37	25
PUMA (Pual 1986)	24	19
Cylindrical pantograph with parallelogram mechanism	18	9

5. CONCLUSION

In this paper the mechanical efficiency and kinematics of a six-d.o.f., pantograph type manipulators were studied. The mechanical efficiencies of pantograph type manipulators and conventional open-chain and closed-chain type manipulators were evaluated using the concept of modified geometric work. The mechanical efficiency of pantograph type manipulators was found to be the highest. The kinematics of both Cartesian and cylindrical type pantograph manipulators was studied. Two special mechanisms which simplify the kinematics of pantograph type manipulators were introduced. The computational complexity of the kinematics of pantograph type manipulators with these special mechanisms was evaluated and compared with a PUMA type manipulator.

ACKNOWLEDGEMENT

The financial support of the national Science Foundation through the Presidential Young Investigator Award Grant No. DMC 8657920 and the Office of Advanced Engineering Study of the University of Illinois at Chicogo is gratefully acknowledged.

REFERENCES

GCA Corp., 1982, "PT 500-R510 Industrial manual"., St. Paul, USA.

GUPTA, K. C., 1981, "A Note on Position Analysis of Manipulators", Proc. of 7th Applied Mechanisms Conf., pp. 2. 1~2.3, Kansas City, USA.

Hirose, S. and Umetani, Y., 1980, "The Basic Motion Regulation System for a Quadruped Walking Machine", ASME Paper 80-DET-34.

Hirose, S., 1984, "A Study of Design and Control of a Quadruped Walking Vehicle", The International Journal of Robotics Research, Vol. 3, No. 2, pp. 113~133.

Hollerbach, J.M. and Sahar, G., 1983, "Wrist-Partitioned, Inverse Kinematic Accelerations and Manipulator Dynamics", The International Journal of Robotics Research, Vol. 2, No. 4, pp. 61~76.

Hobson, E.W. et. al., 1953, "Squaring the Circle and Other Monographs", New York : Chelsa.

Hunt, K.H., 1986, "The Particular or the General? (Some Examples from Robot Kinematics)". Mechanisms and Machine Theory, Vol. 21, No. pp. 481~487.

Kesseis, J.J., Rambaut, J.P. and Penne, J., 1981, "Walking Robot Multi-Level Architecture and Implementation", Proc. of 4th CISM-IFTOMM Symposium on Theory and Practice of Robot and Manipulators, pp. 297~304, Warsaw, poland.

Paul, R.P. and Zhang, H., 1986, "Computationally Efficient Kinematics for Manipulators with Spherical Wrists Based on the Homogeneous Transformation Representation", The International Journal of Robotics Research, Vol. 5, No. 2, pp. 32~44.

Song, S.M., Waldron, K.J. and Kinzel, G.L., 1985 "Computer-Aided Geometric Design of Legs for a Walking Machine", Mechanisms and Machine Theory, Vol. 20, pp. 587 ~598.

Song, S.M., Lee, J.K. and Waldron, K.J., 1987, "Motion Study of Two and Three Dimensional Pantograph Mechanism", Mechanism and Machine Theory, Vol. 22, pp. 321 ~331.

Song, S.M., and Lin, Y.J., 1987, "Dynamics of Pantograph Type Manipulators", Proc. of 1987 IEEE International Conf. on Robotic and Automation, pp. 456~463, Raleigh, USA.

Waldron, K.J., and Kinzel, G.L., 1981, "The Relationship Between Actuator Genmetry and Mechanical Efficiency in Robots", Proc. of 4th CISM-IFTOMM Symp. Theory and Practice Robots and Manipulators, Amesterdam : Elsevier, pp. 366~374, Zaborow, Poland.

Whitney, D.E., 1972, "The Mathematics of Coordinate Control of Prosthetic Arms and Manipulators", Journal of Dynamic Systems, Measurement, and Control, pp. 303~309.

Yang, D.C.H. and Lin, Y.Y., 1985, "Pantograph Mechanism as a Non-Traditional Manipulator Structure", Mechanism and Machine Theory, Vol. 20, No. 2, pp. 115~122.

Appendix

Referring to Fig. 13, the position of the hand reference point F is :

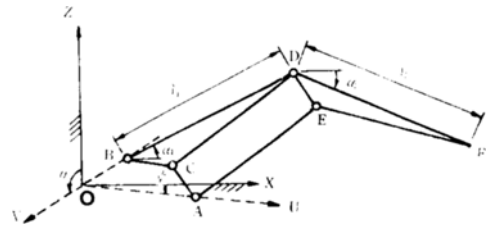

Fig. 13 Link attitude of a planar pantograph

$$X_F = X_A + l_1 \cdot \cos\alpha_1 + l_2 \cdot \cos\alpha_2 \tag{48}$$

$$Z_F = Z_B + l_1 \cdot \sin\alpha_1 + l_2 \cdot \sin\alpha_2 \tag{49}$$

where

$$X_A = U \cdot \cos\psi \qquad Z_B = V \cdot \sin\theta$$
$$X_I = U \cdot R_1 \qquad Z_F = V \cdot R$$

Move all the terms which do not contain α_1 to the left. Square both sides of Eqs. (48) and (49) and add these two equation together. Rearranging the remaining terms gives the following equations :

$$A \cdot \cos\alpha_2 + B \cdot \sin\alpha_2 + C = 0 \tag{50}$$

where

$$A = -2U \cdot l_2 (R' - \cos\psi)$$
$$B = -2V \cdot l_2 (R - \cos\theta)$$
$$C = U^2 (R_1 - \cos\psi)^2 + V^2 (R - \cos\theta)^2 - l_1^2 + l_2^2$$

Let

$$\cos\alpha_2 = \{1 - \tan^2(\alpha_2/2)\}/\{1 + \tan^2(\alpha^2/2)\}$$

and

$$\sin\alpha_2 = \{2\tan(\alpha_2/2)\}/\{1 + \tan^2(\alpha_2/2)\}.$$

Substituting these equations into Eq. (50) gives

$$\alpha_2 = 2 \cdot \tan^{-1}\left(\frac{-B - (A^2 + B^2 - C^2)^{\frac{1}{2}}}{A - C}\right) \tag{51}$$